Experimental Evaluation of Stressed Timber Bridge Systems

L. SHELTON BARGER, JR., ROBERTO LOPEZ-ANIDO, AND HOTA V. S. GANGARAO

The stiffness and transverse load distribution variations of stressed timber bridge systems, including the shear lag phenomenon for the Tee and Box superstructure configurations, two stringer spacings, and two prestress levels, were examined. The tests were carried out for static loads that were applied at midspan on both interior and exterior stringer locations. Deflections and strains at different transverse locations on the deck and stringers were obtained. The analysis of the data provides helpful information to evaluate stiffnesses of stressed Tee and Box timber bridges. Composite moments of inertia of the stringers were obtained from the experimental flexibility coefficients. Shear lag in flanges was evaluated by accounting for the effective flange width of an individual composite beam. The experimental strain variations were used to validate this model.

Modern stressed timber bridges have proved to be an efficient and cost-competitive alternative to conventional bridge construction. In the field, 2- to 4-in.-thick lumber laminations that are dried and treated with creosote are squeezed by high-strength steel rods to develop a stress-laminated timber deck. Interlaminar frictional forces are induced on the lumber lamination faces by the compressive or prestressing (squeezing) forces. These frictional forces are responsible for preventing vertical slippage of the lumber laminations (*1*).

A properly designed and fabricated stress-laminated timber deck is economical and safe for bridges with spans of less than 9 m (30 ft) (*2*). Stressed timber bridges of greater span lengths are feasible by adding stringers or beams to a stressed deck. A variety of manufactured timber beams such as laminated veneer lumber, glulam, and parallam can be used for stringers. Therefore stressed timber systems for spans longer than 9 m (30 ft) are possible by modifying the basic stressed deck component with the inclusion of timber stringers to the stressed deck at certain intervals (Tee system) or stringers and a bottom deck (Box system), as shown in Figure 1.

Although the stress-lamination method of building timber bridges has some significant advantages over traditional timber bridge construction, the use of timber for bridges has some limitations that we should address. A stress-laminated system is structurally orthotropic. In the transverse direction, the large number of laminations across the width reduces the transverse stiffness to a small fraction of the longitudinal stiffness. The objective of this study is to understand the stiffness and transverse load distribution variations of the stressed timber systems, including the shear lag phenomenon for the Tee and Box superstructure configurations, for two stringer spacings, and for two prestress levels. The tests described in this paper consisted of static loads applied at midspan on both interior and exterior stringer locations. Deflections and strains at different transverse locations on the deck and stringers were obtained. The analysis of the data from 16 tests provides helpful information for the evaluation of the actual stiffness of Tee and Box stressed timber bridges. Linear regression analyses were conducted on the experimental deflections to compute flexibility coefficients. Composite moments of inertia of the stringers were obtained from the flexibility coefficients. The shear lag phenomenon is accounted for, in a design-oriented approach, by computing the effective flange width of an isolated composite beam. The experimental strain variations were used to validate this model.

Department of Civil Engineering, West Virginia University, Morgantown, W.Va. 26506-6101.

TEST METHODOLOGY AND CONFIGURATIONS

The static testing of scale model Tee and Box stressed systems without creosote treatment was conducted in the Major Units Laboratory at West Virginia University. All the systems were made of northern red oak decks (Grade 3) of nominal 5- × 15-cm (2- × 6-in.) laminations and southern pine glulam beams (24F-V3, SP/SP) 6.10 m (20 ft) long and 62.5 × 12.7 cm (24.625 × 5 in.). The moduli of elasticity (MOE) for the bridge components were obtained from the linear portion of the load-deflection curve following the Standard Methods of Static Tests of Timbers in Structural Sizes (ASTM D198-84). The mean MOE obtained for the northern red oak boards was E_D = 11 170 MPa (1,620,000 psi), with a coefficient of variation of 15.3 percent. The mean MOE obtained for the southern pine glulam beams was E_S = 9060 MPa (1,314,000 psi).

Tee and Box systems with a span L = 5.89 m (19 ft 4 in.) were built with two different stringer configurations. The three-stringer models had a center-to-center stringer spacing S = 135 cm (53 in.), and the four-stringer models had S = 81 cm (32 in.). A predetermined butt joint pattern of one butt joint every four laminations was used to assemble the decks. The actual deck thickness was 14 cm (5.5 in.). A good approximation for the deck longitudinal modulus was the mean MOE obtained for the boards (E_D) (*3*). Each model was tested with two prestress levels: 0.690 MPa (100 psi) and 0.345 MPa (50 psi).

Midspan deflections and strains were obtained at different transverse locations on the decks and on the stringers. The deflections and strains were measured with LVDTs and strain gauges, respectively, at load increments of 4.45 kN (1,000 lb).

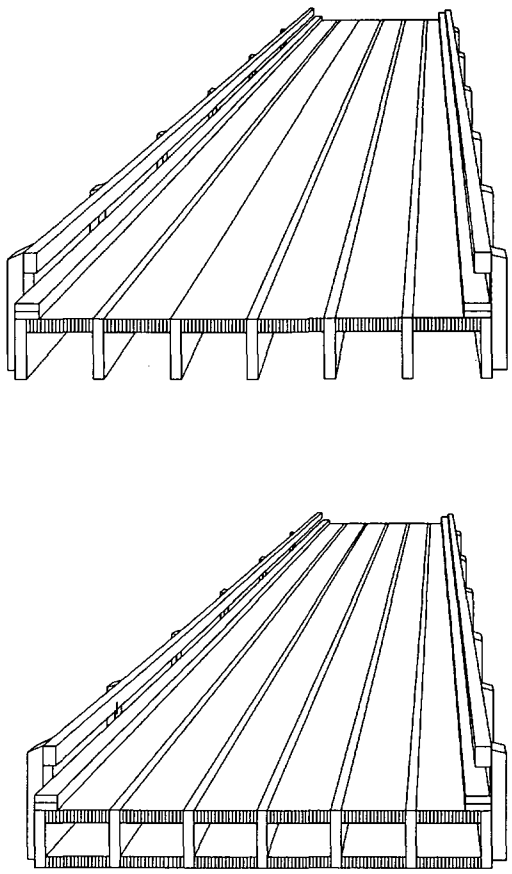

FIGURE 1 Typical stress-laminated timber bridges: *top*, Tee system; *bottom*, Box system.

The loading was applied with a hydraulic ram and measured by a calibrated load cell. The applied load cases for each configuration included a concentrated load on an interior stringer and a concentrated load on an exterior stringer. The concentrated load was applied over an area of 20 × 14 cm (8 × 5.5 in.). The transverse prestress level of the decks was monitored during the tests.

ANALYSIS OF EXPERIMENTAL DEFLECTIONS AND EVALUATION OF TRANSVERSE LOAD DISTRIBUTION FACTORS

Load-deflection (P-δ_i) curves for the models at the lower stress level under a load applied on an interior stringer are shown in Figure 2. The reductions in flexibility from a Tee to a Box system and from a three- to a four-stringer configuration can be seen in Figure 2. Flexibility coefficients (δ_i/P) were obtained from linear regression analyses on the experimental deflections and are presented in Tables 1 and 2 for the three- and four-stringer models, respectively. The results from Tables 1 and 2 allow us to evaluate the flexibility response of the models at different transverse locations and under different loading conditions. Maximum flexibility coefficients for the Box models are approximately 87 percent of the corresponding values for the Tee models at an interior stringer and 78 percent at an exterior stringer.

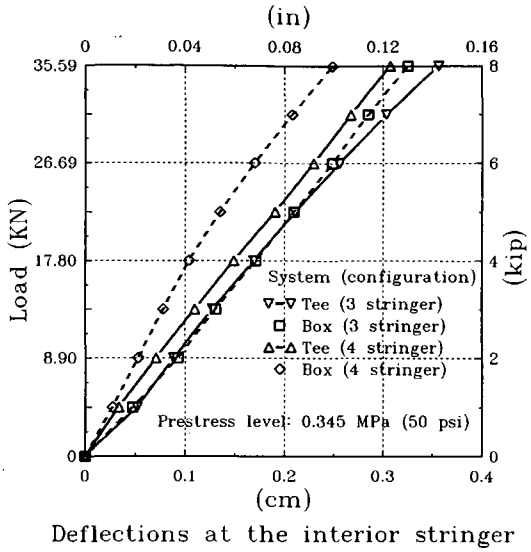

FIGURE 2 Load-deflection curves for the models at the lower stress level under a load applied on an interior stringer.

The transverse load distribution is evaluated at the ith stringer location by computing the following factor:

$$\omega_i = \frac{\left(\frac{\delta_i}{P}\right)_{EXP}}{\sum_{j=1}^{N}\left(\frac{\delta_j}{P}\right)_{EXP}} \quad (1)$$

where the flexibility coefficients $(\delta_i/P)_{EXP}$ are obtained from Tables 1 and 2 and N is the number of stringers. The transverse load distribution factors ω_i for different tests are presented in Table 3. Maximum ω_i's for the four-stringer Box model are about 85 percent of the corresponding factors for the Tee model at an interior stringer and 81 percent at an exterior stringer. The increment in maximum ω_i from an interior to an exterior stringer is around 17 percent for the Tee system and 12 percent for the Box system. A reduction in stringer spacing of 40 percent from the three- to the four-stringer models yields a decrease in maximum ω_i of roughly 19 percent for the Tee system and 27 percent for the Box system.

ANALYSIS OF EXPERIMENTAL STRAINS AND INVESTIGATION OF THE SHEAR LAG EFFECT

Load-strain curves for the three-stringer models under a concentrated load applied on the interior stringer are shown in Figure 3. After an initial slack, a linear relation is observed in the range of 8.90 kN (2,000 lb) to 26.69 kN (6,000 lb). The transverse variations of experimental strains under a load P = 17.80 kN (4,000 lb) applied on the interior stringer are plotted in Figure 4 for the three-stringer models and in Figure 5 for the four-stringer models. In the upper deck, a nonuniform compressive strain distribution is observed, and it is more pronounced for the Tee than for the Box system. A severe local effect in the variation of the tensile strains is noted in

TABLE 1 Flexibility Coefficients for the Three-Stringer Models[a]

Load location	Prestress level (MPa)	Tee δ_1/P (mm/KN)	Tee δ_2/P (mm/KN)	Box δ_1/P (mm/KN)	Box δ_2/P (mm/KN)
#1[b]	0.690	0.1144	0.0059	0.0873	0.0163
	0.345	0.1242	0.0066	0.1048	0.0147
#2[c]	0.690	0.0076	0.0842	0.0084	0.0760
	0.345	0.0055	0.0937	0.0070	0.0878

[a]Obtained from linear regression on the experimental curves of load versus deflection.
[b]Concentrated load applied on exterior stringer #1.
[c]Concentrated load applied on interior stringer #2.
1 MPa = 145.04 psi
1 mm = 0.0394 in
1 KN = 224.81 lbs

TABLE 2 Flexibility Coefficients for the Four-Stringer Models[a]

Load location	Pre-stress level (MPa)	Tee δ_1/P (mm/KN)	Tee δ_2/P (mm/KN)	Tee δ_3/P (mm/KN)	Tee δ_4/P (mm/KN)	Box δ_1/P (mm/KN)	Box δ_2/P (mm/KN)	Box δ_3/P (mm/KN)	Box δ_4/P (mm/KN)
#1[b]	0.690	0.1020	0.0184	0.0050	0.0036	0.0739	0.0292	0.0131	0.0029
	0.345	0.1218	0.0114	0.0023	0.0014	0.0946	0.0218	0.0057	0.0046
#2[c]	0.690	0.0185	0.0820	0.0150	0.0029	0.0251	0.0617	0.0200	0.0068
	0.345	0.0114	0.0902	0.0143	0.0043	0.0154	0.0814	0.0171	0.0040

[a]Obtained from linear regression on the experimental curves of load versus deflection.
[b]Concentrated load applied on exterior stringer #1.
[c]Concentrated load applied on interior stringer #2.
1 MPa = 145.04 psi
1 mm = 0.0394 in
1 KN = 224.81 lbs

TABLE 3 Transverse Load Distribution Factors[a]

System	Prestress Level (MPa)	Three-stringer models: Symmetric interior load ω_1[b]	Three-stringer models: Symmetric interior load ω_2[c]	Four-stringer models: Asymmetric interior load ω_1	ω_2[c]	ω_3	ω_4	Asymmetric edge load ω_1[c]	ω_2	ω_3	ω_4
Tee	0.690	0.07	0.86	0.16	0.69	0.13	0.02	0.79	0.14	0.04	0.03
	0.345	0.05	0.90	0.09	0.75	0.12	0.04	0.89	0.08	0.02	0.01
Box	0.690	0.09	0.82	0.22	0.54	0.18	0.06	0.62	0.25	0.11	0.02
	0.345	0.07	0.86	0.13	0.69	0.15	0.03	0.75	0.17	0.05	0.04

[a]Computed from Equation 1.
[b]Applicable to both exterior stringers due to symmetry.
[c]Evaluated at the location of the concentrated load.
1 MPa = 145.04 psi

the lower deck of the Box models under the applied load. The influence of the prestressing level in the transverse strain distribution can be observed in Figures 4 and 5. Because no slip in between the laminations was observed, the steep strain drop is attributed to the shear lag phenomenon that is more critical in stressed timber bridges than in conventional decks. This inability of the stressed deck to transmit shear stresses reduces the "effective width" in a stressed timber deck design.

EVALUATION OF COMPOSITE BEAM STIFFNESS AND COMPUTATION OF THE EFFECTIVE FLANGE WIDTH

In the design of a Tee or a Box stressed timber bridge, it is necessary to evaluate the composite moment of inertia of an individual beam formed by the stringer and the effective portion of the deck. Composite beam moments of inertia for the

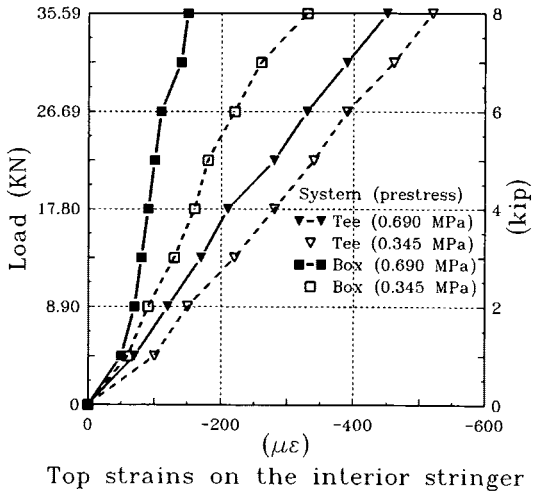

FIGURE 3 Load-strain curves for the three-stringer models under a load applied on the interior stringer.

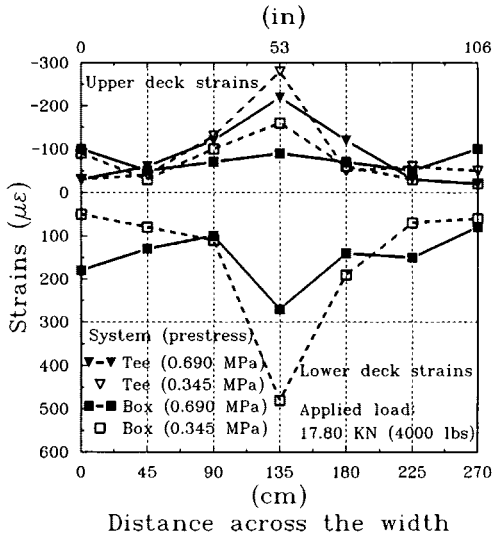

FIGURE 4 Transverse strain distribution for the three-stringer models under a load applied on the interior stringer.

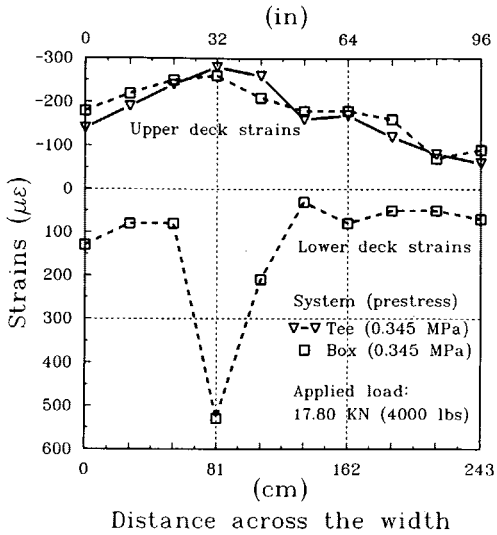

FIGURE 5 Transverse strain distribution for the four-stringer models at the lower stress level under a load applied on an interior stringer.

different configurations were obtained by equating the experimental flexibility coefficients from Tables 1 and 2 with the corresponding normalized beam deflection formula modified by the appropriate load distribution factor from Table 3. Then for the ith stringer we get

$$I_C = \frac{L^3}{48E_S}\frac{\omega_i}{\left(\frac{\delta_i}{P}\right)_{EXP}} = \frac{L^3}{48E_S}\frac{1}{\sum_{j=1}^{N}\left(\frac{\delta_j}{P}\right)_{EXP}} \quad (2)$$

The resulting composite moments of inertia I_C are presented in Table 4 relative to the stringer inertia I_S. The Box systems develop an increment in I_C with respect to the corresponding Tee systems by about 4 percent for interior stringers and 8 percent for exterior stringers.

Regarding the design of a timber bridge system as an isolated composite beam, the reduction in the collaborating deck width due to the shear lag effect was evaluated. Total effective flange widths (b_E) were obtained from the composite moments of inertia by assuming an equivalent homogeneous T-

TABLE 4 Composite Moment of Inertia[a] and Effective Flange Width[b]

System	Prestress level (MPa)	Three-stringer models[c] Interior stringer #2 I_C / I_S	b_E / S	Four-stringer models[d] Interior stringer #2 I_C / I_S	b_E / S	Exterior stringer #1 I_C / I_S	b_E / S
Tee	0.690	1.85	0.37	1.53	0.38	1.41	0.31
	0.345	1.74	0.32	1.51	0.37	1.33	0.28
Box	0.690	1.96	0.18	1.59	0.25	1.52	0.24
	0.345	1.78	0.17	1.54	0.24	1.44	0.22

[a]Computed from Equation 2, and expressed relative to the stringer inertia.
[b]Obtained from the composite moment of inertia by assuming an equivalent homogeneous section, and expressed relative to the stringer spacing.
[c]Spacing center to center of stringers: S = 135 cm.
[d]Spacing center to center of stringers: S = 81 cm
1 MPa = 145.04 psi
1 cm = 0.394 in

section for the Tee systems and an equivalent homogeneous I-section for the Box systems. The resulting effective flange widths are given in Table 4 relative to the stringer spacing. The reduction in effective width of an exterior stringer relative to an interior stringer is more pronounced for the Tee system (22 percent) than for the Box system (6 percent). The variation of effective deck width with the level of prestressing is about 9 percent for the Tee models and 6 percent for the Box models. The four-stringer Box system presents an effective width that is around 65 and 78 percent of the corresponding values of the Tee system for an interior and an exterior stringer, respectively. The reduction in effective flange width for the Box configurations is justified because of the more pronounced shear lag developed in the bottom deck in the proximity of the load location, as shown in Figures 4 and 5. For the four-stringer Tee system the effective width can be expressed as 1/20 of the span or 2.2 times the deck thickness, whereas for the Box system the effective width can be stated as 1/30 of the span or 1.4 times the deck thickness. The effective flange widths computed in Table 4 account for the influence of the butt joint pattern in the deck.

CONCLUSIONS

From our experimental data, and as preliminary design guidelines for a Tee system, the effective flange width of S/3 for the interior stringers and S/4 for the exterior stringers are recommended. Similarly, for the Box system, effective flange widths of S/4 for the interior stringers and S/5 for the exterior stringers are recommended. In the field, over a long period of time, we expect the prestress level to stabilize near 0.345 MPa (50 psi). For this reason, we recommend this prestress level for design purposes. In the field the diaphragms effectively contribute to increase the transverse stiffness of the Tee system. The curbs also provide a substantial stiffening of the exterior stringers. These effects, which yield a better transverse load distribution leading to higher load sharing by the exterior stringers, have been excluded from the results reported in this paper and will be presented as a sequel to this study. Effects due to loads applied between stringers will also be discussed in a separate paper.

The analysis of the data provides helpful information for the evaluation of the stiffness of stressed Tee and Box timber bridges, including the transverse load distribution factors and the effective flange widths. The analysis of the transverse strain variation provides a valuable insight toward the understanding of the reported results. Mathematical models representing the above behavior of Tee and Box systems are being developed and will be presented as an extension of this study.

ACKNOWLEDGMENT

The research presented in this paper was sponsored by FHWA. The authors appreciate the valuable comments of the reviewers and Sheila Duwadi of FHWA.

REFERENCES

1. Dickson, B. D., and H. V. S. GangaRao. Development and Testing of an Experimental Timber T-Beam Bridge. In *Transportation Research Record 1275,* TRB, National Research Council, Washington, D.C., 1990.
2. GangaRao, H. V. S., and I. Latheef. System Innovation and Experimental Evaluation of Stressed Timber Bridges. *Proc., 1991 International Timber Engineering Conference,* TRADA, London, Vol. 3, 1991, pp. 3.327–3.334.
3. Brokaw, J. T., and J. F. Davalos. *Strength and Stiffness Properties for Stress-Laminated Timber Decks.* Report CFC-92-TR157. Constructed Facilities Center, West Virginia University, Morgantown, 1992.

The contents of this paper reflect the views of the authors and do not reflect the official views of the sponsor.